

## Electrostatic Properties of Membrane Lipids Coupled to Metarhodopsin II Formation in Visual Transduction

Yin Wang,<sup>†,‡</sup> Ana Vitória Botelho,<sup>§</sup> Gary V. Martinez,<sup>||</sup> and Michael F. Brown<sup>\*,§,||</sup>

Contribution from the Departments of Physics, Biochemistry and Molecular Biophysics, and Chemistry, University of Arizona, Tucson, Arizona 85721

Received January 9, 2002

**Abstract:** Changes in lipid composition have recently been shown to exert appreciable influences on the activities of membrane-bound proteins and peptides. We tested the hypothesis that the conformational states of rhodopsin linked to visual signal transduction are related to biophysical properties of the membrane lipid bilayer. For bovine rhodopsin, the meta I–meta II conformational transition was studied in egg phosphatidylcholine (PC) recombinants versus the native rod outer segment (ROS) membranes by means of flash photolysis. Formation of metarhodopsin II was observed by the change in absorbance at 478 nm after a single actinic flash was delivered to the sample. The meta I/meta II ratio was investigated as a function of both temperature and pH. The data clearly demonstrated thermodynamic reversibility of the transition for both the egg PC recombinants and the native ROS membranes. A significant shift of the *apparent*  $pK_a$  for the acid–base equilibrium to lower values was evident in the egg PC recombinant, with little meta II produced under physiological conditions. Calculations of the membrane surface pH using a Poisson–Boltzmann model suggested the free energies of the meta I and meta II states were significantly affected by electrostatic properties of the bilayer lipids. In the ROS membranes, phosphatidylserine (PS) is needed for full formation of meta II, in combination with phosphatidylethanolamine (PE) and polyunsaturated docosahexaenoic acid (DHA; 22:6 $\omega$ 3) chains. We propose that the PS surface potential leads to an accumulation of hydronium ions,  $H_3O^+$ , in the electrical double layer, which drive the reaction together with the large negative *spontaneous curvature* ( $H_0$ ) conferred by PE plus DHA chains. The elastic stress/strain of the bilayer arises from an interplay of the  $\sim$  zero  $H_0$  from PS and the negative  $H_0$  due to the PE headgroups and polyunsaturated chains. The lipid influences are further explained in terms of matching of the bilayer spontaneous curvature to the curvature at the lipid/rhodopsin interface, as formulated by the Helfrich bending energy. These new findings guide current ideas as to how bilayer properties govern the conformational energetics of integral membrane proteins. Moreover, they yield knowledge of how membrane lipid–protein interactions involving acidic phospholipids such as PS and neutral polyunsaturated DHA chains are implicated in key biological functions such as vision.

### Introduction

Recently, substantial evidence has accumulated showing that variations in phospholipid composition can affect cellular processes involving integral membrane proteins.<sup>1</sup> In the case of vision, rod outer segment (ROS)<sup>2</sup> membranes containing the transmembrane protein rhodopsin can be studied as a model to understand and interpret the role of membrane lipids in protein activity.<sup>3</sup> Further, rhodopsin constitutes a useful example with

regard to the chemical biology of membrane receptors whose functions include cellular regulatory mechanisms involving heterotrimeric G proteins.<sup>4,5</sup> The crystal structure of rhodopsin has been determined at 2.8 Å resolution, making it the first G protein-coupled receptor (GPCR) to be investigated at the atomic level by X-ray diffraction.<sup>6</sup> Rhodopsin is an attractive paradigm for studies of GPCRs in general, as the protein is naturally labeled with a chromophoric group, 11 *cis*-retinal,<sup>7</sup> its functional states are well-defined spectroscopically,<sup>8</sup> and it is the major protein constituent of the rod disk membranes.<sup>9</sup> In addition, rhodopsin can be recombined with various natural and synthetic

\* To whom correspondence should be addressed. Phone: 520-621-2163. Fax: 520-621-8407. E-mail: mfbrown@u.arizona.edu.

<sup>†</sup> Department of Physics.

<sup>‡</sup> Present address: Department of Biology, University of California at San Diego, La Jolla, CA 92093-0366.

<sup>§</sup> Department of Biochemistry and Molecular Biophysics.

<sup>||</sup> Department of Chemistry.

(1) Dowhan, W. *Annu. Rev. Biochem.* **1997**, *66*, 199–232.

(2) Abbreviations: DHA, docosahexaenoic acid; DOPC, dioleoylphosphatidylcholine; DOPE, dioleoylphosphatidylethanolamine; egg PC, egg yolk phosphatidylcholine; GPCR, G protein-coupled receptor; meta I or MI, metarhodopsin I; meta II or MII, metarhodopsin II; PC, phosphatidylcholine or phosphocholine; PE, phosphatidylethanolamine or phosphoethanolamine; PS, phosphatidylserine or phosphoserine; PMT, photomultiplier tube; ROS, rod outer segment.

(3) Brown, M. F. *Curr. Top. Membr.* **1997**, *44*, 285–356.

(4) Liebman, P. A.; Parker, K. R.; Dratz, E. A. *Annu. Rev. Physiol.* **1987**, *49*, 765–791.

(5) Salamon, Z.; Brown, M. F.; Tollin, G. *Trends Biochem. Sci.* **1999**, *24*, 213–219.

(6) Palczewski, K.; Kumasaka, T.; Hori, T.; Behnke, C. A.; Motoshima, H.; Fox, B. A.; Le Trong, I.; Teller, D. C.; Okada, T.; Stenkamp, R. E.; Yamamoto, M.; Miyano, M. *Science* **2000**, *289*, 739–745.

(7) Nakanishi, K.; Crouch, R. *Isr. J. Chem.* **1995**, *35*, 253–272.

(8) Kliger, D. S.; Lewis, J. W. *Isr. J. Chem.* **1995**, *35*, 289–307.

(9) Hofmann, K. P.; Jäger, S.; Ernst, O. P. *Isr. J. Chem.* **1995**, *35*, 339–355.

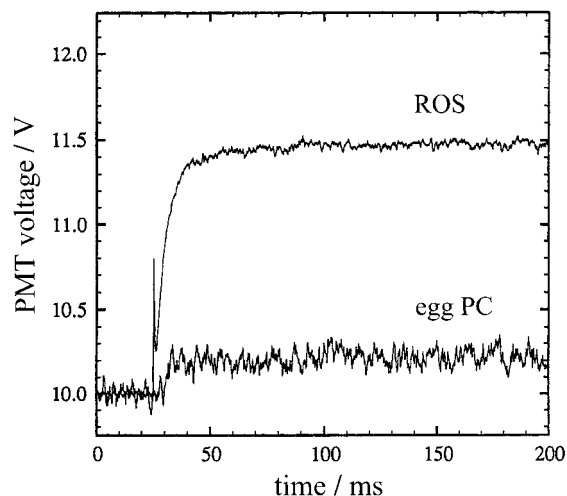


**Figure 1.** Photomultiplier (PMT) voltage output at 478 nm following a single actinic flash for rhodopsin/egg PC (1:100) recombinant membranes versus native ROS membranes, measured at pH 7.0 and  $T = 28\text{ }^{\circ}\text{C}$ . The phototransients indicate the dependence of the meta I–meta II equilibrium on the membrane environment.

phospholipids to yield recombinant membranes which have been shown to be fully active in terms of their photochemistry.<sup>10</sup> Alteration of the retinal chromophore,<sup>7</sup> site-directed mutation of rhodopsin,<sup>11</sup> and membrane lipid substitution<sup>10,12–14</sup> have all been shown to yield significant changes in functional parameters.

In visual signal transduction, 11-*cis* to -*trans* isomerization of the retinal chromophore leads to activation of rhodopsin embedded within the membrane, which is followed by switching on the G protein (transducin) and its effector proteins to yield the biological response.<sup>3,9</sup> The key triggering event is believed to be the meta I–meta II conformational transition of photolyzed rhodopsin.<sup>4,9</sup> Many previous studies of the meta I–meta II transition have focused on rhodopsin in the native ROS membranes.<sup>8</sup> Current emphasis has centered about the effects of site-directed mutagenesis of rhodopsin on its function when studied in detergent micelles.<sup>11,15,16</sup> Yet it is not always recognized that equally dramatic influences on the meta I–meta II transition can arise from alteration of the membrane lipid environment of wild-type rhodopsin.<sup>10,13,14,17</sup> Using an *in vitro* approach, recombinants of rhodopsin can be studied with various phospholipids to gain a better understanding of the role of the lipid bilayer properties in triggering the visual process. Here the egg phosphatidylcholine (PC) recombinant, having a single lipid headgroup type together with unsaturated acyl chains, constitutes a reference system to which other rhodopsin-containing membranes can be compared.<sup>14</sup> By determining the metarhodopsin I–metarhodopsin II ratio produced by flash photolysis, the role of phospholipids in the visual signal can be investigated systematically.<sup>3</sup> As an illustrative example, consider the flash photolysis data shown in Figure 1. Clearly, rhodopsin in the egg PC recombinant membranes shows a substantial

reduction in the postflash transmittance signal versus the native ROS membranes. What is the origin of this striking alteration of the photochemistry of rhodopsin? Additional experiments reveal that a natively like lipid composition, comprising phosphatidylcholine, phosphatidylethanolamine (PE), and phosphatidylserine (PS), together with docosahexaenoic acid (DHA) chains, is sufficient for a full meta I–meta II transition. Yet lipid substitution experiments<sup>14,17</sup> also indicate that such a lipid mixture is unnecessary, suggesting the importance of material properties of the bilayer. For neutral lipid mixtures, the key property may involve the elastic stress/strain associated with deformation of the membrane bilayer.<sup>17</sup> Moreover, studies of the influences of PS headgroups<sup>18</sup> suggest that electrostatic properties of the bilayer lipids are important. A related finding is that phosphorylation of rhodopsin<sup>19</sup> increases the *apparent*  $pK_a$  for the meta I–meta II equilibrium, due to the negative surface charge in rod disk membranes. Other work has considered the topology of rhodopsin in terms of an electrostatic model of the disk membrane, which describes the net charge at the membrane surface.<sup>19,20</sup>

We have now carried out a more detailed comparison of the photochemistry of rhodopsin in the native ROS membranes to the reference egg PC recombinant at different temperatures and pH values to further explore the role of biophysical properties of the bilayer. Our objective was to test the hypothesis that the local pH of the ROS membranes, due to the presence of the negatively charged PS headgroups, shifts the meta I–meta II transition of rhodopsin.<sup>14,18</sup> Additional influences of neutral lipids, for example, due to polyunsaturated DHA chains or PE headgroups, can thus be identified. Following refs 14, 19, and 20, we have considered the meta I–meta II equilibrium as a function of the *local* pH, *viz.*, within the electrical double layer, as well as the *bulk* pH. By applying the Gouy–Chapman model, the intrinsic  $pK_a$  values can be compared. This work indicates a significant electrostatic contribution to metarhodopsin II formation in the ROS membranes. Our principal finding is that the surface potential due to PS headgroups leads to an increased local  $[\text{H}_3\text{O}^+]$ , which can quantitatively account for the enhanced meta II in the native ROS membranes versus the reference egg PC recombinant. Moreover, the presence of PS counteracts or antagonizes the influences of the neutral PE headgroups plus DHA chains in the native ROS membranes, which also favor meta II. As an explanation, we suggest that the surface charge density due to PS alters the deformation energy associated with elastic curvature stress/strain of the bilayer, which is proposed as a free energy coupling mechanism in the retinal rod membranes.<sup>17</sup> Finally, we point out that the electrostatic contribution alone does not explain the influences of lipid bilayer diversity on rhodopsin activity. These findings indicate a complex interplay of the bilayer electrostatic properties with elastic membrane deformation in governing receptor activation in the visual system.

## Experimental and Theoretical Procedures

**Preparation of Retinal Rod Membranes and Recombinants with Phospholipids.** Native ROS membranes were prepared from frozen bovine retinas (W. L. Lawson, Co., Lincoln, NE) as described.<sup>21</sup> They

(10) Wiedmann, T. S.; Pates, R. D.; Beach, J. M.; Salmon, A.; Brown, M. F. *Biochemistry* **1988**, *27*, 6469–6474.

(11) Khorana, H. G. *Proc. Natl. Acad. Sci. U.S.A.* **1993**, *90*, 1166–1171.

(12) Baldwin, P. A.; Hubbell, W. L. *Biochemistry* **1985**, *24*, 2624–2632.

(13) Mitchell, D. C.; Straume, M.; Miller, J. L.; Litman, B. J. *Biochemistry* **1990**, *29*, 9143–9149.

(14) Gibson, N. J.; Brown, M. F. *Biochemistry* **1993**, *32*, 2438–2454.

(15) Sakmar, T. P.; Fahmy, K. *Isr. J. Chem.* **1995**, *35*, 325–337.

(16) Jäger, S.; Lewis, J. W.; Zvyaga, T. A.; Szundi, I.; Sakmar, T. P.; Klinger, D. S. *Proc. Natl. Acad. Sci. U.S.A.* **1997**, *94*, 8557–8562.

(17) Brown, M. F. *Chem. Phys. Lipids* **1994**, *73*, 159–180.

(18) Gibson, N. J.; Brown, M. F. *Biochem. Biophys. Res. Commun.* **1991**, *176*, 915–921.

(19) Gibson, S. K.; Parkes, J. H.; Liebman, P. A. *Biochemistry* **1999**, *38*, 11103–11114.

(20) Tsiu, F. C.; Sundberg, S. A.; Hubbell, W. L. *Biophys. J.* **1990**, *57*, 85–97.

were osmotically shocked by suspension in water, followed by centrifugation (2–4 $\times$ ) to remove the G protein (transducin) and other associated peripheral membrane proteins, and stored in 67 mM sodium phosphate buffer, pH 7.0, at  $-70^{\circ}\text{C}$ . All manipulations were carried out in dim red light (15 W bulb; Kodak Safelight filter no. 1) at  $4^{\circ}\text{C}$ . Rhodopsin was purified by column chromatography on hydroxyapatite (Bio-Rad Laboratory, DNA grade Bio-Gel HTP, Hercules, CA) having a  $2.5 \times 6.5$  cm final bed.<sup>22</sup> The column was equilibrated with 100 mM of the detergent dodecyltrimethylammonium bromide (Sigma, St. Louis, MO), 15 mM sodium phosphate, pH 6.8, and 1 mM dithiothreitol at  $4^{\circ}\text{C}$ . A linear gradient of 0.0–0.5 M NaCl was used to elute rhodopsin. To recombine rhodopsin with egg PC (Avanti Polar Lipids, Alabaster, AL), the phospholipids in chloroform were argon-dried in a glass round-bottom flask, then vacuum-dried overnight to constant weight. The dried egg PC was weighed to determine a 100:1 lipid/protein molar ratio in the final recombinants. The chloroform-free lipid was solubilized in detergent, mixed with rhodopsin, and incubated for 45 min at  $4^{\circ}\text{C}$ . The mixture was dialyzed for 48 h against 5 mM Hepes buffer containing 1 mM EDTA at pH 6.8 ( $0.5 \text{ L mg}^{-1}$  rhodopsin), under a constant nitrogen stream, changing the dialysis buffer every 4 h.<sup>22</sup> Before conducting the flash photolysis experiments, both the native ROS membranes and the rhodopsin/egg PC recombinants were exchanged into 10 mM of the appropriate buffer by several cycles of centrifugation followed by resuspension. Sodium phosphate was typically used for the pH range 4.5–9.0. Titration data over an extended range of pH utilized the following buffers: sodium citrate, sodium acetate, sodium borate, and sodium glycinate. UV–visible absorption spectra were recorded with a Varian 2290 spectrophotometer as described.<sup>14</sup> The typical  $A_{280}/A_{500}$  absorbance ratio for the ROS native membranes was 2.4–2.7, and for the rhodopsin/egg PC recombinants it was 1.6–1.8.

**Flash Photolysis Measurements.** Prior to the flash data acquisition, sonicated samples of either ROS membranes or rhodopsin/egg PC recombinants were prepared in 10 mM sodium phosphate buffer at the desired pH to yield a rhodopsin concentration of  $2.2 \mu\text{M}$ . Sonication was carried out (Heat Systems-Ultrasonics, Inc., model W375, Plainview, NY) using a microtip at  $\sim 25\%$  maximum power, in an ice bath with a 50% duty cycle for 3 min under argon, to reduce the light scattering of the samples. The bulk solution pH was measured both before and after the experiments by inserting the pH electrode directly into the flash photolysis cuvette. Typically, the pH values differed by less than 0.1 units. The data were acquired using a home-built, single-beam kinetic spectrophotometer.<sup>10,14,23</sup> The instrument was set up to monitor changes in light transmission at 478 nm, the absorption maximum for metarhodopsin I, with a sampling interval of  $50 \mu\text{s}$ , and a total acquisition time of 400 ms. After delivering a single actinic flash, the PMT voltage change ( $\Delta V$ ) was obtained from the difference of the postflash and preflash voltage. The transient signal monitored the formation of meta II from the mixture of rhodopsin and meta I produced within the instrument dead time ( $\sim 30 \mu\text{s}$ ). UV–visible spectrophotometry was used to determine the absorbance change at 500 nm relative to the nonflashed ROS membrane control, thereby providing a measure of the degree of bleaching each time the sample was exposed to the actinic flash.<sup>14</sup> A flash transient was recorded after the first flash, and following multiple flashes repeatedly delivered to the sample, until no change in the output voltage was observed. This provided a record of the scattered flash lamp afterglow.

The results can, in principle, depend on the membrane preparation as well as optical parameters of the flash photolysis setup, so that appropriate control studies are essential. For instance, the various sonicated membrane preparations scattered light away from the detector

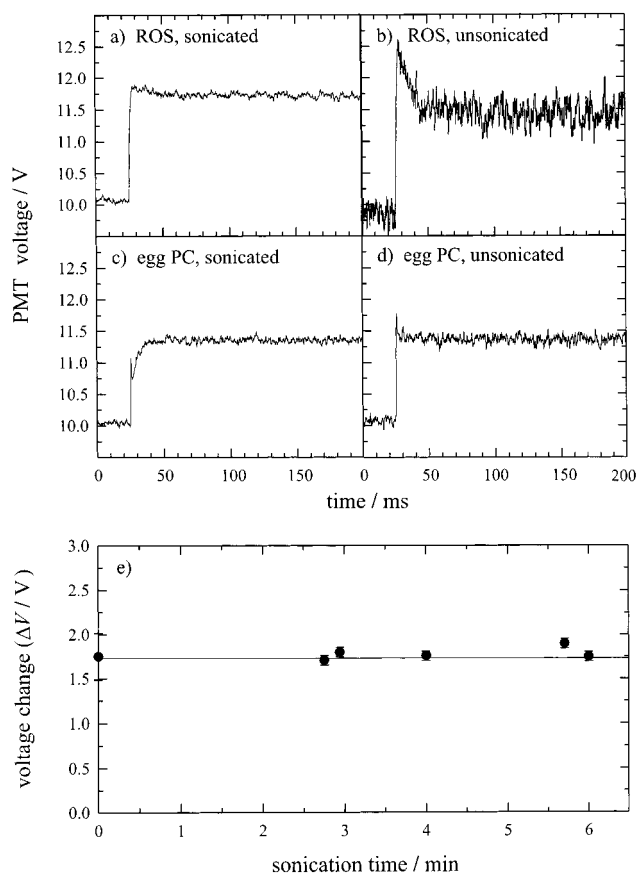


**Figure 2.** Control flash photolysis studies at 478 nm demonstrating the influences of membrane size: (a), (b) sonicated versus unsonicated ROS membranes; and (c), (d) sonicated versus unsonicated rhodopsin/egg PC (1:100) recombinant membranes, each at pH 5.0 and  $T = 28^{\circ}\text{C}$ . In all cases the effects of light scattering were compensated by adjusting the PMT gain (cf. text). (e) Plot of PMT voltage change for the native ROS membranes against the time of sonication at pH 5.0 and  $T = 28^{\circ}\text{C}$ . Data are the averages of multiple measurements. Note that the PMT voltage change is essentially independent of the sonication time.

to a varying degree. This was corrected by adjusting the photoelectrical gain, which is controlled by the voltage across the PMT. In our experiments, the preflash PMT output voltage offset was adjusted to a constant value of 10 V for each of the measurements to correct for the variable degree of light scattering of the samples and the accuracy of the optical path alignment.<sup>14</sup> If the influences of light scattering are properly compensated, then the sonication procedure should not appreciably change the magnitudes of the phototransients. To confirm that this was indeed the case, control studies were performed for various sample suspensions, with representative data for the ROS membranes and the egg PC recombinants at pH 5.0 shown in Figure 2. Comparison of part a with part b, and part c with part d, indicates that the final amplitudes of the flash transient signals were not greatly influenced by the procedure. However, the noise for the sonicated samples was substantially less due to reduction of the light scattering. In addition, variations in the scattered flash lamp afterflow gave an initial artifact for the more strongly scattering samples, which resulted from the increased PMT gain, cf. Figure 2b. The influences of the sonication time were further tested with representative data for the ROS membranes shown in Figure 2e. The data indicate that the PMT output voltage changes are essentially constant after correction for light scattering. Moreover, consistent results were obtained using different preparations of the native and recombinant membranes, as described below.

**Reduction and Analysis of Flash Photolysis Data.** Quantitative analysis of the meta II intermediate produced by flash photolysis was

(21) Papermaster, D. S.; Dreyer, W. J. *Biochemistry* **1974**, *13*, 2438–2444.

(22) Hong, K.; Hubbell, W. L. *Biochemistry* **1973**, *12*, 4517–4523.

(23) Beach, J. M.; Pates, R. D.; Ellena, J. F.; Brown, M. F. *Biophys. J.* **1984**, *45*, 292a.

carried out from the acquired photomultiplier output voltage change ( $\Delta V$ ). This was converted to an absorbance change ( $\Delta A$ ), and then to the mole fraction of meta II ( $\theta$ ) produced after the flash. For the purpose of data analysis, we assumed a simple acid–base equilibrium<sup>24</sup> for the overall meta I–meta II transition, viz.,  $\text{MI} + \nu\text{H}_3\text{O}^+ \rightleftharpoons \text{MII}$ , using  $\nu = 1$ .<sup>19</sup> The changes in transmittance at 478 nm following the actinic flash were assumed to be due solely to the fraction of rhodopsin photolyzed, and the conversion of meta I to meta II. A molar absorption coefficient was taken for rhodopsin of  $\epsilon_{498}^{\text{rho}} = 40\,600\text{ M}^{-1}\text{ cm}^{-1}$  at 498 nm,<sup>25</sup> with a value of  $\epsilon_{478}^{\text{rho}} = 37\,000\text{ M}^{-1}\text{ cm}^{-1}$  estimated from the experimental absorption spectrum.<sup>14</sup> The meta I intermediate was assumed to have a molar absorption coefficient of  $\epsilon_{478}^{\text{MI}} = 44\,000\text{ M}^{-1}\text{ cm}^{-1}$  at 478 nm.<sup>26</sup> The absorption at 478 nm due to meta II was assumed to be  $\sim 0$ . The postflash change in absorbance at 478 nm,  $\Delta A_{478}$ , was obtained directly from the voltage difference signal using the Beer–Lambert law:

$$\Delta A = \log(V_0/V_{\text{postflash}}) - \log(V_0/V_{\text{preflash}}) \quad (1a)$$

$$= \log(V_{\text{preflash}}/V) - \log(V_{\text{preflash}}/V + \Delta V/V) \quad (1b)$$

The above equations reduced to

$$\Delta A = 1 - \log(10 + \Delta V/V) \quad (2)$$

after adjusting the preflash voltage to the constant value of 10 V (vide supra). For each experiment, the absorbance values at 500 nm in the presence of  $\text{NH}_2\text{OH}$  were used to calculate the percentage of rhodopsin bleached, given by

$$f = 1 - \frac{A_{500}^{\text{postflash}} - A_{500}^{\text{bleached}}}{A_{500}^{\text{preflash}} - A_{500}^{\text{bleached}}} \quad (3)$$

In the above expression,  $f$  is the fraction of bleached rhodopsin,  $A_{500}^{\text{postflash}}$  is the residual absorption of the flashed sample at 500 nm,  $A_{500}^{\text{preflash}}$  is the absorption of the sample before the actinic flash, and  $A_{500}^{\text{bleached}}$  is the absorption of the fully bleached sample.<sup>14</sup> For the fitting lines in the graphs, the following equation was used:

$$\Delta A_{478} = (1 - \theta)\Delta A_{478}^{\text{MI}} + \theta\Delta A_{478}^{\text{MII}} \quad (4)$$

in which  $\Delta A_{478}^{\text{MI}} = \Delta\epsilon_{478}^{\text{MI}}[\text{rho}]_0 l$  and  $\Delta A_{478}^{\text{MII}} = \Delta\epsilon_{478}^{\text{MII}}[\text{rho}]_0 l$ , where  $[\text{rho}]_0 \equiv f[\text{rho}]_{\text{init}}$ , that is, corresponding to the limiting absorbance change, and the path length  $l = 5\text{ cm}$ . The first term of eq 4 was substituted either with zero for  $\Delta\epsilon_{478}^{\text{MI}}$ , or  $\Delta\epsilon_{478}^{\text{MI}} = 7000\text{ M}^{-1}\text{ cm}^{-1}$ , with  $\Delta\epsilon_{478}^{\text{MII}} = -37\,000\text{ M}^{-1}\text{ cm}^{-1}$  (vide supra). Least-squares fits to the data employed the downhill simplex method, as implemented in Matlab (The MathWorks, Inc., Natick, MA). The mole fraction of photolyzed rhodopsin in the metarhodopsin II form was obtained using eq 4, yielding

$$\theta = 0.159 - 2.07 \frac{\Delta A_{478}}{f} \quad (5)$$

An additional important aspect is that multiple photon events can occur so that variations in the efficiency of photobackreaction of bathorhodopsin, lumirhodopsin, or meta I can affect the apparent yield of meta II (cf. Figure 1). To eliminate this possibility, further control studies of the actinic light intensity were conducted. According to the above treatment, cf. eq 5, the mole fraction of meta II ( $\theta$ ) should be independent of the percentage of rhodopsin bleached. Representative control experiments to confirm this prediction are shown in Figure 3

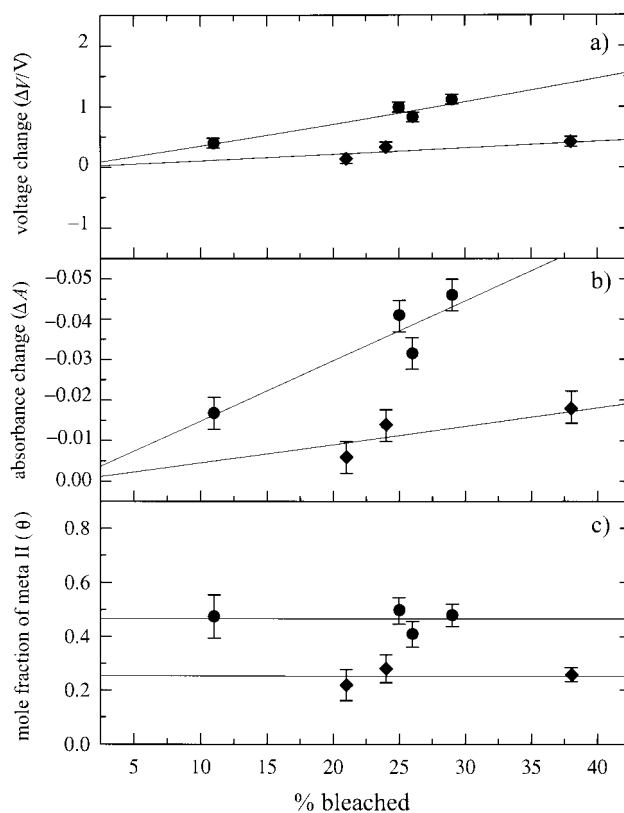


**Figure 3.** Flash photolysis control studies at 478 nm showing effect of actinic flash intensity for rhodopsin/egg PC (1:100) recombinants at  $T = 28\text{ }^\circ\text{C}$ : (●) pH 6.0; (◆) pH 8.0 ( $\pm 0.1$ ). (a) Postflash PMT voltage change ( $\Delta V$ ); (b) absorbance change ( $\Delta A$ ); and (c) mole fraction of meta II ( $\theta$ ). The percentage of rhodopsin bleached was controlled using neutral density filters and monitored by UV–visible spectrophotometry. Data points and error bars correspond to multiple measurements. The mole fraction of meta II is essentially independent of the actinic light intensity up to nearly 40% rhodopsin bleached.

for the egg PC recombinant membranes at  $T = 28\text{ }^\circ\text{C}$  and pH values of 6.0 and 8.0. Parts a and b indicate that the voltage change ( $\Delta V$ ) and absorbance change ( $\Delta A$ ) are proportional to the percentage of rhodopsin bleached following a single actinic flash. This implies that the ratio of  $\Delta A$  to the fraction of rhodopsin bleached ( $f$ ) is constant, under the same conditions of  $T$ , pH, in accord with eq 5. Generally, a value of  $f \approx 25\% \equiv 0.25$  was used in this work to maximize the signal-to-noise, while keeping multiple photon events to a minimum.<sup>10</sup> One can conclude from the control experiments that the photomultiplier signal following the actinic flash is a direct response of the protein to the properties of the membrane lipid environment.

**Thermodynamic Model.** In what follows, we consider a simple thermodynamic treatment of the conformational energetics of integral membrane proteins such as rhodopsin. It is useful to begin with the fundamental equation of chemical thermodynamics

$$dG = V dP - S dT + \sum_i \mu_i dn_i \quad (6)$$

where all symbols have their conventional meanings:  $G$  is the Gibbs free energy,  $V$  the total volume,  $P$  the total pressure,  $S$  the entropy, and  $T$  the temperature. In dealing with biochemical equilibria, for example, the meta I–meta II transition of rhodopsin, it is important to provide an accurate definition of the standard states. The chemical potentials are

$$\mu_i = \left( \frac{\partial G}{\partial n_i} \right)_{T,P,n_{j \neq i}} = \mu_i^\circ + \gamma_i \left( \frac{m_i}{m_i^\circ} \right) \quad (7)$$

(24) Parkes, J. H.; Liebman, P. A. *Biochemistry* **1984**, *23*, 5054–5061.

(25) Applebury, M. L.; Hargrave, P. A. *Vision Res.* **1986**, *26*, 1881–1895.

(26) Applebury, M. L.; Zuckerman, D. M.; Lamola, A. A.; Jovin, T. M. *Biochemistry* **1974**, *13*, 3448–3458.

where  $n_i$  is the moles of the  $i$ th component,  $\gamma_i$  is the activity coefficient,  $m_i$  is the molality, and the Henry's law standard state (superscript  $^\circ$ ) is assumed. Dividing  $dG$  by the differential extent of reaction  $d\xi$  at constant  $T, P$  yields

$$\Delta G = \left( \frac{\partial G}{\partial \xi} \right)_{T,P} = \sum_i \nu_i \mu_i \quad (8)$$

in which  $\nu_i$  are the (signed) stoichiometric coefficients of the products (+) and reactants (-).

One can then consider the overall meta I–meta II equilibrium of rhodopsin following flash photolysis



The chemical potentials are given by

$$\mu_{\text{MI}} = \mu_{\text{MI}}^\circ + RT \ln[\text{MI}] \quad (10a)$$

$$\mu_{\text{MII}} = \mu_{\text{MII}}^\circ + RT \ln[\text{MII}] \quad (10b)$$

$$\mu_{\text{H}} = \mu_{\text{H}}^\circ + \nu RT \ln[\text{H}_3\text{O}^+] = \mu_{\text{H}}^\circ - 2.303\nu RT \text{pH} \quad (10c)$$

where the square brackets [ ] indicate the component activities, viz.,  $\gamma_i(m_i/m^\circ)$ . From eqs 8 and 10a–10c, the equilibrium constant for the meta I–meta II transition is<sup>14</sup>

$$K = e^{-\Delta G^\circ/RT} = \frac{[\text{MII}]_{\text{eq}}}{[\text{MI}]_{\text{eq}}[\text{H}_3\text{O}^+]_{\text{eq}}^\nu} \quad (11)$$

corresponding to the *base* ionization constant, which is independent of pH. The dependence of the fraction of meta II formed ( $\theta$ ) on pH is given by

$$\theta = \frac{[\text{MII}]_{\text{eq}}}{[\text{MI}]_{\text{eq}} + [\text{MII}]_{\text{eq}}} = \frac{1}{1 + 10^{\nu \text{pH} + \text{p}K}} \quad (12)$$

In eq 12,  $\text{p}K = -\text{p}K_a$ , where  $K_a$  is the *acid* ionization constant corresponding to the inverse of the equilibrium in eq 9. (We have previously reported  $\text{p}K$  values for the meta I–meta II equilibrium<sup>14</sup> as the midpoint pH.) In what follows, values of  $\text{p}K_a$  ( $= -\text{p}K$ ) are given. Note that use of the *bulk* solution pH in the above expression gives the *apparent*  $\text{p}K_a$  for the transition. However, for a titratable surface, the dependence of the local pH on the surface potential leads to a shifting and broadening of the titration curve ( $\nu \neq 1$ ). Alternatively, use of the *local* pH (calculated from the surface potential; vide infra) yields a Henderson–Hasselbalch titration curve in terms of the *intrinsic*  $\text{p}K_a$ . It is also possible to include multiple equilibria, for example, more complex reaction mechanisms,<sup>9,27–29</sup> involving isochromic forms of meta II such as meta II<sub>a</sub> and meta II<sub>b</sub>.

To include a description of electrostatic influences on the meta I–meta II equilibrium, the Gouy–Chapman equation was used to calculate the surface (local) pH of the membrane.<sup>30,31</sup> The above treatment can be further extended in terms of the electrochemical potential,  $\mu_i$ , by including the electrostatic potential  $\psi$ , leading to

$$\mu_i \rightarrow \bar{\mu}_i \equiv \mu_i + \mu_i^{\text{el}} \quad (13)$$

where  $\mu_i^{\text{el}} = z_i F \psi$  is the electrical energy,  $z_i$  is the ion charge, and  $F$  is the Faraday constant. Equating the electrochemical potential for

hydronium ions, eq 13, at the membrane surface ( $\psi = \psi_0$ ) and in the bulk solution ( $\psi = 0$ ) yields the Nernst equation

$$\text{pH}_{\text{local}} = \text{pH}_{\text{bulk}} + \frac{zF\psi_0}{2.303RT} \quad (14)$$

(Strictly speaking, pH is a property of the bulk solution so that one should refer to the local  $\text{H}_3\text{O}^+$  concentration.) The electrostatic potential is related to the surface charge density ( $\sigma$ ) in terms of the Poisson–Boltzmann equation, which for a planar surface gives the Gouy–Chapman formula

$$\sigma = \left( \frac{C^{1/2}}{A} \right) \sinh \left( \frac{zF\psi_0}{2RT} \right) \quad (15)$$

Here  $\sigma$  is the membrane surface charge density,  $\psi_0$  is the membrane surface potential,  $C$  is the molarity of cations due to the sodium phosphate buffer,  $z = 1$  is the sodium ion charge, and  $A = 134.8 \text{ M}^{1/2} \text{ \AA}^2$ . Note that in eq 15 the electrical potential  $\psi_0$  is not an additive function, whereas the surface charge density can be decomposed into lipid and protein components

$$\sigma = \sigma^{\text{L}} + \sigma^{\text{P}} \quad (16)$$

The lipid<sup>32</sup> and protein<sup>19,20</sup> contributions have been discussed previously.

Alternatively, the total charge density per rhodopsin unit cell, eq 16, can be calculated using

$$\sigma = -\sigma_{\text{PS}} + \sum_i \sigma_{\text{basic}}^{(i)} - \sum_j \sigma_{\text{acidic}}^{(j)} \quad (17)$$

Following refs 19 and 20, the charge density of PS is obtained from the formula

$$\sigma_{\text{PS}} = \frac{N}{1 + \left( \frac{[\text{H}_3\text{O}^+]}{K_{\text{H}}} + \frac{[\text{Na}^+]}{K_{\text{salt}}} \right) \exp \left( -\frac{F\psi_0}{RT} \right)} \quad (18)$$

Here  $N$  is the surface density of the ionizable groups, assuming a surface area for a rhodopsin unit cell of  $4000 \text{ \AA}^2$  at  $T = 28 \text{ }^\circ\text{C}$ ,<sup>4,20</sup>  $K_{\text{H}}$  is the dissociation constant for  $\text{H}_3\text{O}^+$ ,  $K_{\text{salt}} = 1/0.7 \text{ M}$  is the dissociation constant for binding of  $\text{Na}^+$  to PS, and  $[\text{H}_3\text{O}^+]$  and  $[\text{Na}^+]$  are the bulk concentrations of the hydronium and sodium ions (in the phosphate buffer solution).<sup>19</sup> The *intrinsic*  $\text{p}K_a$  value<sup>33</sup> used for the PS carboxyl group was 3.6. The contribution from the charge density of the basic amino acids is given by

$$\sigma_{\text{basic}}^{(i)} = \frac{N}{1 + 10^{\text{pH}_{\text{local}} - \text{p}K_a(i)}} \quad (19)$$

where  $K_a(i)$  is the corresponding acid ionization constant of the  $i$ th residue. For the acidic amino acids

$$\sigma_{\text{acidic}}^{(j)} = N \left( 1 - \frac{1}{1 + 10^{\text{pH}_{\text{local}} - \text{p}K_a(j)}} \right) \quad (20)$$

The Gouy–Chapman model, eq 15, and the directly calculated charge density, eq 17, yield a set of simultaneous, nonlinear equations which can be solved iteratively for the surface potential  $\psi_0$ . The *local* pH is then obtained from the *bulk* pH using the Nernst equation, eq 14.

We also introduce in this work the biochemical standard state (superscript  $^\circ$ ), corresponding to a one molar total concentration of all ionized species at the standard pH at which the sample is buffered, for example, pH 7. The purpose is to enable the contribution from

(27) Hofmann, K. P. *Photobiochem. Photobiophys.* **1986**, *13*, 309–327.

(28) Jäger, S.; Szundi, I.; Lewis, J. W.; Mah, T. L.; Kliger, D. S. *Biochemistry* **1998**, *37*, 6998–7005.

(29) Okada, T.; Ernst, O. P.; Palczewski, K.; Hofmann, K. P. *Trends Biochem. Sci.* **2001**, *26*, 318–324.

(30) McLaughlin, S. *Curr. Top. Membr. Transp.* **1977**, *9*, 71–144.

(31) Cevc, G. *Biochim. Biophys. Acta* **1990**, *1031*, 311–382.

(32) Hubbell, W. L. *Biophys. J.* **1990**, *57*, 99–108.

(33) Tsui, F. C.; Ojcius, D. M.; Hubbell, W. L. *Biophys. J.* **1986**, *49*, 459–468.

hydronium ions to the free energies of the meta I and meta II states to be separated from the other free energy terms, so that the thermodynamic results are independent of the stoichiometry of  $\text{H}_3\text{O}^+$  in the equilibrium. All possible isochromic forms of metarhodopsin I and metarhodopsin II, for example, meta II<sub>a</sub> and meta II<sub>b</sub>, are summed to give a single thermodynamic component, viz., meta II, and the standard part of their chemical potential  $\mu_i^{\circ'}$  is assumed to be approximately equal to the Henry's law value  $\mu_i^{\circ}$ . For hydronium ions  $\mu_{\text{H}^+}^{\circ'} = \mu_{\text{H}^+}^{\circ} + \nu RT \ln \gamma_{\text{H}^+}(m^{\circ'}/m^{\circ})$ , which at pH 7.0 yields  $\mu_{\text{H}^+}^{\circ'} = \mu_{\text{H}^+}^{\circ} + 16.1\nu RT$ . This gives a pseudo-equilibrium constant which is pH-dependent:<sup>14</sup>

$$K'_{\text{pH}} = e^{-\Delta G^{\circ'}/RT} = \frac{[\text{MII}]_{\text{eq}}}{[\text{MI}]_{\text{eq}}} = \frac{\theta}{1 - \theta} \quad (21)$$

The data for the temperature dependence of the absorbance change,  $\Delta A_{478}$ , were fit using eq 4 together with

$$\theta = \frac{1}{1 + e^{-\Delta S^{\circ'}/R} e^{+\Delta H^{\circ'}/RT}} \quad (22)$$

where  $\Delta S^{\circ'}$  and  $\Delta H^{\circ'}$  are the entropy and enthalpy changes for the meta I–meta II transition assuming biochemical standard states. With this convention, the standard part of the chemical potential, viz., the part independent of the protein and hydronium ion concentrations (activities), can be further decomposed as follows:

$$\mu_i^{\circ} = \mu_i^{\circ\text{L}} + \mu_i^{\circ\text{LP}} + \mu_i^{\circ\text{P}} \quad (23)$$

where  $i \equiv \text{MI}, \text{MII}$ . The standard-state chemical potential includes contributions from the lipid bilayer (L), the lipid–protein interface (LP), and the protein (P), as discussed previously.<sup>3,14,17</sup>

## Results

**The Meta I–Meta II Transition Is Shifted in Recombinants with Egg Phosphatidylcholine.** The flash photolysis studies employed recombinant egg PC membranes having a lipid/rhodopsin molar ratio of 100:1. This ratio was chosen to be roughly similar to the native bovine ROS membranes, with a lipid/rhodopsin ratio<sup>34</sup> of  $\sim 75:1$ . As rhodopsin is by far the major protein component of the osmotically shocked and water-washed ROS membrane preparations ( $>99$  mol %),<sup>21</sup> differences between the samples are associated with the membrane lipid bilayer. The rhodopsin/egg PC recombinant membranes were studied over a wide range of pH at 28 °C, and multiple preparations were used, as also in the case of the ROS membranes. Representative flash photolysis transients for the egg PC recombinant and the native ROS membranes are given above. The smaller flash photolysis signals at neutral pH for the egg PC recombinant versus the ROS membranes (Figure 1) are due to a decrease in formation of the metarhodopsin II state. This is not a result of the different lipid/rhodopsin molar ratios, since additional control studies of rhodopsin/egg PC recombinants evince a modest reduction of only  $\sim 10\%$  in the mole fraction of meta II with an increase from 75 to 100 lipids/rhodopsin.<sup>35</sup> Consequently, the output voltage signals indicate that the *apparent*  $\text{pK}_a$  for the meta I–meta II transition is decreased substantially in the rhodopsin/egg PC (1:100) recombinant versus the native ROS membranes.

An illustration of the initial reduction and analysis of the flash photolysis data is provided in Figure 4. The postflash PMT

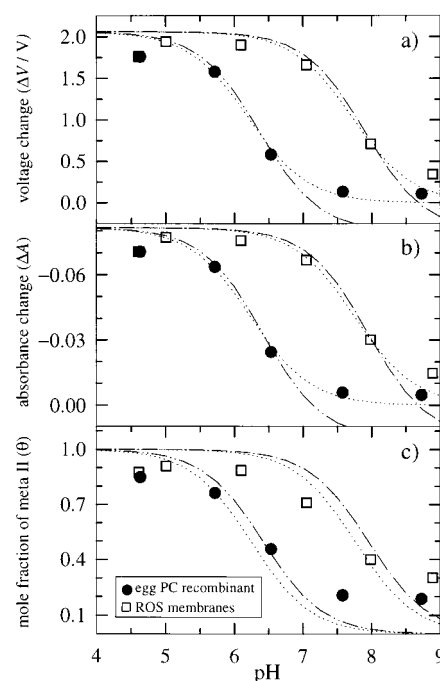


**Figure 4.** Reduction and analysis of flash photolysis data at 478 nm for rhodopsin/egg PC (1:100) recombinant membranes (●) and native ROS membranes (□). (a) Photomultiplier voltage change ( $\Delta V$ ); (b) absorption change ( $\Delta A$ ); and (c) mole fraction of meta II ( $\theta$ ) generated by a single actinic flash as a function of pH at  $T = 28$  °C. Data points are the average of multiple measurements. Illustrative fits are to guide the eye and assume a two-state acid–base equilibrium ( $f = 20\%$ ), either neglecting the absorbance change at 478 nm due to meta I (···) or assuming a positive absorbance change (---). A shift of the pH titration curve is clearly evident for the rhodopsin/egg PC (1:100) recombinant ( $\text{pK}_a = 6.4 \pm 0.2$ ) as compared to the native ROS membranes ( $\text{pK}_a = 7.8 \pm 0.3$ ).

output voltage change ( $\Delta V$ ), absorbance change ( $\Delta A$ ), and mole fraction of metarhodopsin II ( $\theta$ ) are plotted for a single series of experimental measurements against the bulk solution pH in parts a–c, respectively. Because the photochemical activity is higher at acid pH, an uptake of protons occurs in conjunction with the meta I–meta II conformational change.<sup>9,19,36,37</sup> Note that full activity of rhodopsin is obtained at acidic pH values in both the native ROS membranes and the rhodopsin/egg PC (1:100) recombinant membranes. As an initial approximation, the experimental data were fit simultaneously to a simple titration equilibrium using eqs 2, 4, and 12. (A bleached fraction of  $f = 20\%$  was found to fit the titration data better than the average value of  $\sim 25\%$ .) First, the contribution from the meta I intermediate to the absorbance change was neglected, yielding a zero end point at the basic pH values (dotted line), and, second, an increase in absorption at 478 nm due to meta I was assumed (dashed line). As compared to a simple Henderson–Hasselbalch equilibrium, in either case a broadening of the titration curves is evident, which is further considered below. There is some uncertainty as to the residual meta II at basic pH values, due to the possibility of light scattering changes following photolysis.<sup>27,38</sup> However, an important finding at this juncture is that the *apparent*  $\text{pK}_a$  calculated for the meta I–meta II transition is different for the egg PC recombinant as compared to the native

(36) Thorgeirsson, T. E.; Lewis, J. W.; Wallace-Williams, S. E.; Kliger, D. S. *Biochemistry* **1993**, *32*, 13861–13872.

(37) Gibson, N. J.; Brown, M. F. *Biochem. Biophys. Res. Commun.* **1990**, *169*, 1028–1034.

(38) Hofmann, K. P.; Uhl, R.; Hoffmann, W.; Kreutz, W. *Biophys. Struct. Mech.* **1976**, *2*, 61–77.

(34) Stone, W. L.; Farnsworth, C. C.; Dratz, E. A. *Exp. Eye Res.* **1979**, *28*, 387–397.

(35) Wang, Y. Ph.D. Dissertation, University of Arizona, 1997.

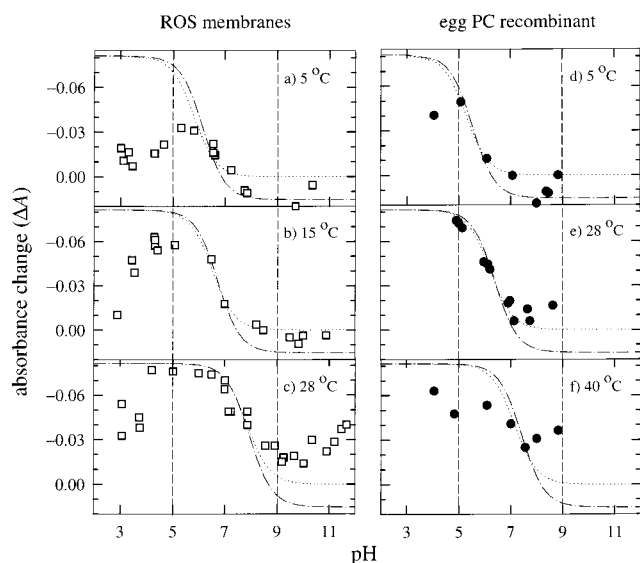


**Figure 5.** Summary of flash photolysis results showing absorbance change ( $\Delta A$ ) at 478 nm following a single actinic flash over an extended pH range: (a)–(c) ROS membranes ( $\square$ ) at  $T = 5, 15,$  and  $28\text{ }^{\circ}\text{C}$ , respectively; (d)–(f) rhodopsin/egg PC (1:100) recombinant membranes ( $\bullet$ ) at  $T = 5, 28,$  and  $40\text{ }^{\circ}\text{C}$ , respectively. The vertical dashed lines represent the range of pH over which an approximately sigmoidal transition is seen. Fits to the (unaveraged) data for pH 5–9 ( $f = 20\%$ ) neglect the absorbance change at 478 nm due to meta I ( $\cdots$ ), or include a positive absorbance change (---). At lower and higher pH values, further changes are evident (cf. text).

ROS membranes. The main effect of the perturbation due to egg PC is a substantial shift in the apparent  $pK_a$  for the acid–base equilibrium to lower values. These results show that at physiological pH the photochemical activity of the rhodopsin/egg PC recombinant is dramatically less than in the native ROS membranes.

The temperature and pH dependencies for the rhodopsin meta I–meta II transition in the native ROS membranes and the egg PC recombinant membranes are summarized in Figure 5, where the postflash absorbance changes are plotted over an expanded range of bulk pH. Similar results are obtained for the postflash PMT voltage ( $\Delta V$ ) and for the mole fraction of meta II ( $\theta$ ) (not shown). The experimental results clearly deviate from a simple titration equilibrium either at the lower pH values, below about pH 4.5, or higher than about pH 9.0, for instance at 28 and 40  $^{\circ}\text{C}$ . More or less, sigmoidal titration behavior is observed when the apparent  $pK_a$  falls roughly midway between the pH range of about 5–9, near the rhodopsin isoelectric point<sup>39</sup> of  $pI = 6.0$ . Comparing the data to a simple acid–base equilibrium, the broadening and deviation at acidic and basic pH values can be attributed to the more complex processes of an amphoteric membrane surface, or to pH-induced denaturation of rhodopsin. The former is associated with the electrostatic potential due to the titratable amino acid residues of the protein, as well as the membrane lipid surface charge (from PS in ROS), which can lead to a broadening of the titration curve.<sup>19,20</sup> The decrease at acid pH values is possibly due to protonation of the  $\text{COO}^-$  groups of Asp and Glu residues of rhodopsin or the lipid PS headgroups. At the basic pH values, deprotonation of Cys SH, Lys  $\text{NH}_3^+$ , and Tyr OH groups together with the PS and PE headgroups of the lipids can occur.<sup>20,33</sup> Additionally, the existence of a high pH form of bovine rhodopsin<sup>40</sup> may affect

the behavior of the protein at pH values above  $\sim 9.5$ . Clearly, the lipid environmental influences on the rhodopsin photoactivity are quite significant whenever the pH value is close to neutral. As the meta I–meta II transition is an endothermic process, the apparent  $pK_a$  shifts from left to right with increasing temperature. For the ROS membranes at  $T = 5, 15,$  and  $28\text{ }^{\circ}\text{C}$ , parts a–c, assuming a two-state analysis, the data within the pH 5–9 range correspond to apparent  $pK_a$  values of 6.7, 7.0, and 7.8, respectively. The results for the native ROS membranes are consistent with previous data at  $28\text{ }^{\circ}\text{C}$ ,<sup>14</sup> and also with flash photolysis experiments between  $-1$  and  $15\text{ }^{\circ}\text{C}$ .<sup>24</sup> For the rhodopsin/egg PC (1:100) recombinant membranes, parts d–f, apparent  $pK_a$  values of 5.5, 6.3, and 7.2 were found at  $T = 5, 28,$  and  $40\text{ }^{\circ}\text{C}$ , respectively.

#### Influences of Temperature and pH Demonstrate Thermodynamic Reversibility of the Metarhodopsin Equilibrium.

A key aspect of this work involves substantiating that the lipid effects in recombinant membranes are due to a reversible modulation of the meta I–meta II transition, for example, as opposed to inactivation of the protein. Controls for the influences of light scattering and degree of photolysis of rhodopsin are described above. Further evidence in support of a thermodynamically reversible meta I–meta II equilibrium for both the rhodopsin/egg PC (1:100) recombinants and the native ROS membranes is provided in Figure 6. To emphasize the correspondence of different thermodynamic state variables, the absorbance change  $\Delta A$  at  $\lambda = 478\text{ nm}$  is plotted either as a function of pH or against the temperature in the same figure. Part a summarizes additional pH titration data obtained for the meta I–meta II transition of rhodopsin in the ROS membranes and egg PC recombinant at  $T = 28\text{ }^{\circ}\text{C}$ . Fits to the experimental data using eqs 4 and 12 with  $f = 20\%$  are in generally good agreement with the results presented above. The effect of the lipid environment is a translation along the pH axis; it is mainly the midpoint (apparent  $pK_a$ ) that is shifted with similar end points in each case. However, closer inspection indicates deviations from simple Henderson–Hasselbalch pH titration behavior, as noted previously.<sup>14</sup> Part b shows thermal transition data obtained for the ROS membranes and rhodopsin/egg PC recombinant at pH 7.0. Fits to the data using eqs 4 and 22 with  $f = 25\%$  yield  $\Delta H^{\circ} = +42.4 \pm 26.6\text{ kJ mol}^{-1}$  and  $\Delta S^{\circ} = +148 \pm 92.0\text{ J K}^{-1}\text{ mol}^{-1}$  for the ROS membranes; and  $\Delta H^{\circ} = +66.1 \pm 33.3\text{ kJ mol}^{-1}$  and  $\Delta S^{\circ} = +212 \pm 109\text{ J K}^{-1}\text{ mol}^{-1}$  for the rhodopsin/eggPC recombinant membranes, where cross-correlations in the fitting parameters are considered. Here the influence of temperature represents a shifting of the thermal midpoint along the temperature axis, with similar low and high temperature end points corresponding to meta I and meta II, respectively. (Note that the pH and temperature ranges are limited by the stability of rhodopsin.) Hence both the effects of pH and temperature are comparable, and indicate a thermodynamic reversibility of the equilibrium between the meta I and meta II states, as opposed to any degree of irreversible inactivation of the protein. Because the transition can be driven nearly to completion by either a decrease in pH or an increase in temperature, differences in the flash photolysis behavior of rhodopsin in the egg PC recombinant versus the native ROS membranes are due to modulation of the meta I–meta II equilibrium by the lipid composition.

(39) Miller, J. L.; Fox, D. A.; Litman, B. J. *Biochemistry* **1986**, *25*, 4983–4988.

(40) Koutalos, Y. *Biophys. J.* **1992**, *61*, 272–275.

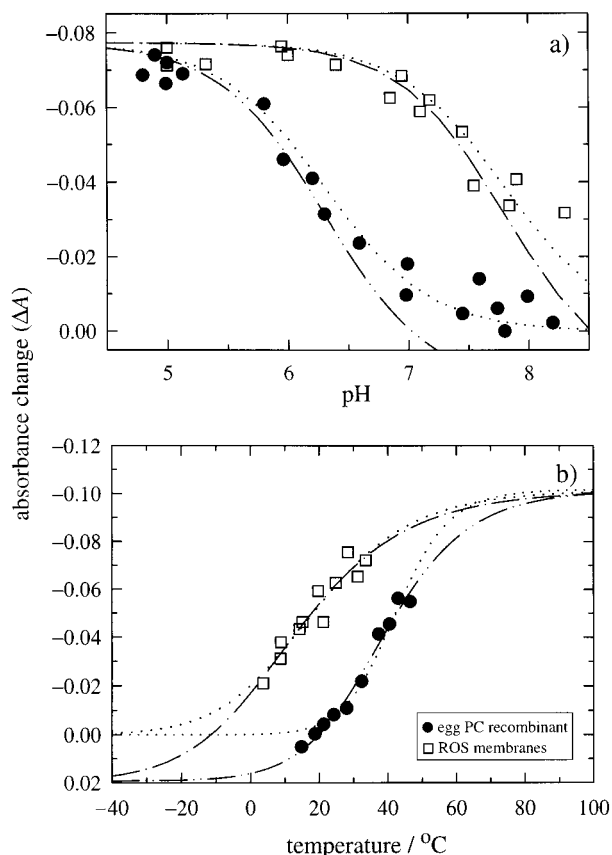


**Figure 6.** Thermodynamic reversibility of the meta I–meta II transition for rhodopsin/egg PC (1:100) recombinant membranes (●) and ROS membranes (□). Flash photolysis results for the absorption change ( $\Delta A$ ) at 478 nm are shown. (a) Comparison of (unaveraged) values of  $\Delta A$  as a function of pH at  $T = 28^{\circ}\text{C}$  together with fits to data ( $f = 20\%$ ). Note the *apparent*  $pK_a$  for the egg PC recombinant is shifted by  $\sim 1.5$  units to a lower value as compared to the ROS membranes. (b) Plots of (unaveraged) values of  $\Delta A$  versus temperature at pH 7.0 with data fits ( $f = 25\%$ ). Here the (partial) thermal transition curve for the egg PC recombinant is displaced  $\sim 25^{\circ}\text{C}$  to higher temperatures relative to the ROS membranes. The data as a function of either pH or temperature imply a reversible shifting of the meta I–meta II equilibrium by the membrane lipid environment.

### Electrostatic Properties of the Membrane Affect the Meta I–Meta II Conformational Change of Rhodopsin.

As mentioned above, one also needs to consider the influences of the bilayer electrostatics in the case of ionic lipids, such as PS, as well as titration of the acidic and basic residues of the amphoteric rhodopsin molecule. Generally, it is necessary to separate the “indirect” influences of the membrane surface potential  $\psi_0$  on the ionic composition of the electrical double layer<sup>20,30</sup> from the “direct” electrostatic influences on the physical state of the bilayer.<sup>17</sup> For instance, in the ROS membranes, the shift of the titration curve to a higher *apparent*  $pK_a$  value versus the egg PC recombinant may come from the effect of the charged headgroups of the membrane, that is, due to accumulation of  $\text{H}_3\text{O}^+$  ions in the electrical double layer adjacent to the membrane surface. In addition, electrostatic interactions can alter parameters such as the rhodopsin net charge, conformation, and mobility of the extramembraneous peptide loops, as well as properties of the membrane bilayer. Although the actual mechanism may be more complex, due to the possibility of isochromic forms<sup>9,29</sup> of meta II, a comparison of the intrinsic  $pK_a$  values obtained in the flash photolysis

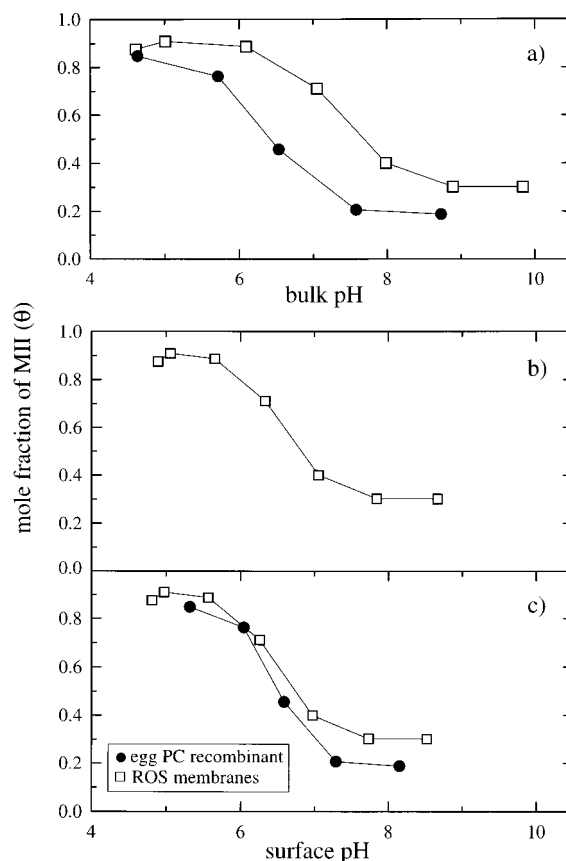


**Figure 7.** Influences of bulk solution pH versus membrane surface pH on meta I–meta II equilibrium of rhodopsin/egg PC (1:100) recombinant membranes (●) and native ROS membranes (□). Flash photolysis results (averaged) are shown for the mole fraction of meta II ( $\theta$ ) in each case. (a) Meta II fraction as a function of *bulk* solution pH measured potentiometrically. (b) Meta II fraction versus the *local* pH of the ROS membranes, calculated by assuming an *asymmetric* transbilayer distribution of the lipid and rhodopsin molecules (intrinsic  $pK_a = 6.9 \pm 0.2$ ) (cf. text). (c) Meta II fraction for the egg PC recombinant and ROS membranes plotted against the *local* pH calculated using the Gouy–Chapman model for a *symmetric* (scrambled) transbilayer distribution of the lipids and rhodopsin (intrinsic  $pK_a = 6.6 \pm 0.1$  and  $6.9 \pm 0.2$ , respectively). Note that for the ROS membranes, only a small difference is seen for the asymmetric and symmetric distributions. In addition, part c shows that the intrinsic  $pK_a$  values for the meta I–meta II transition of rhodopsin in the egg PC recombinant and ROS membranes are nearly the same.

experiments for the native ROS membranes to the synthetic egg PC recombinant can further probe the lipid influences on the conformational energetics of rhodopsin.

In what follows, a more detailed analysis of the flash photolysis data for the rhodopsin/egg PC recombinant membranes and the ROS membranes is considered in terms of the bilayer electrostatic properties. Figure 7a shows representative flash photolysis results for the mole fraction of meta II versus the *bulk* pH of the suspension for the rhodopsin/egg PC recombinant as well as the native ROS membranes. As noted above, as compared to a simple two-state acid–base equilibrium, the pH titration curves are significantly broadened. For each experimental bulk pH value, the Gouy–Chapman theory was used to calculate the membrane surface pH using eqs 14 and 15. The calculations accounted for the surface charge density due to the acidic headgroups of PS, as well as the ionizable basic and acidic amino acid residues of rhodopsin.<sup>19,20</sup> A stoichiometric coefficient for the hydronium ions of  $\nu = 1$  was assumed for simplicity;<sup>19</sup> other values were taken from earlier



work.<sup>19,20</sup> First, a starting value of the local pH was assumed, and eq 14 was used to calculate the surface potential  $\psi_0$ . Knowing the value of  $\psi_0$ , the surface charge density  $\sigma$  was calculated from the Gouy–Chapman equation, eq 15, and compared with the value of  $\sigma$  obtained directly from eq 17 using the various group ionization constants. The  $\chi^2$  difference was minimized to obtain  $\text{pH}_{\text{local}}$ , using the downhill simplex method as described above.

The resultant titration curves for the membrane surface pH are shown in Figure 7b and c. Following ref 19, in part b an asymmetric charge distribution is considered for the ROS membranes, including only the ionizable residues on the cytoplasmic side.<sup>20</sup> Alternatively, in part c a symmetric charge model is considered. Note that for the ROS membranes little influence of the transbilayer charge asymmetry is seen; compare part b with part c. This is consistent with our earlier flash photolysis studies indicating similar behavior for the (asymmetric) ROS membranes and (symmetric) recombinants of rhodopsin with the total ROS phospholipids.<sup>10,14</sup> Parts b and c also show that the titration curves as a function of membrane surface pH become narrower, as expected for a simple titration equilibrium, cf. eq 12. However, there are still deviations from simple Henderson–Hasselbalch behavior at the higher pH values, which might reflect the presence of isochromic meta II forms,<sup>9,29</sup> for example, meta II<sub>a</sub> and meta II<sub>b</sub>, which is under further consideration. For the rhodopsin/egg PC recombinant, apart from the narrowing of the local pH titration curve, only a small difference is evident between the *apparent*  $\text{pK}_a$  value of  $6.4 \pm 0.2$  and the *intrinsic*  $\text{pK}_a$  value of  $6.6 \pm 0.1$ , which are close to the isoelectric point ( $\text{pI} = 6.0$ ) of dark-adapted rhodopsin.<sup>20,39</sup> By contrast, for the native ROS membranes the  $\text{pK}_a$  decreases from an *apparent*  $\text{pK}_a$  value of  $7.8 \pm 0.3$ , that is, for the bulk pH in Figure 7a to an *intrinsic*  $\text{pK}_a$  value of  $6.9 \pm 0.2$  regardless of whether an asymmetric or symmetric charge distribution is considered, cf. parts b and c, respectively. Interestingly, the *intrinsic*  $\text{pK}_a$  calculated for the native ROS membranes is close to that found for the rhodopsin/egg PC (1:100) recombinants, and is consistent with titration of a His residue<sup>41</sup> or possibly Glu<sup>134</sup> as the origin of the pH dependence of the meta I–meta II transition.<sup>29</sup>

## Discussion

The work in this paper clearly shows that the bilayer lipid composition can modulate the photochemical function of rhodopsin in the visual process. Current efforts are directed toward understanding the structural features that lead to formation of the activated metarhodopsin II state,<sup>19,29,42</sup> including exposure of its binding sites for the G protein, transducin, thereby triggering the visual process.<sup>3,7–9,27–29,36,43–45</sup> Within the protein, the retinal chromophore<sup>7</sup> is covalently bound to the opsin polypeptide chain in the dark.<sup>6,46,47</sup> Stimulated absorption of light by retinal in its ground state  $S_0$  yields an excited singlet  $S_1$  state,<sup>48</sup> resulting in 11-*cis* to all-*trans* isomerization within

200 fs.<sup>49</sup> The direct light-induced, chromophore–protein interaction is very strong,<sup>7</sup> and costs most of the absorbed energy.<sup>50</sup> Subsequent redistribution of the energy within the protein leads to the meta I–meta II transition,<sup>8,9,28,29</sup> in which deprotonation of the retinal Schiff base linkage occurs. The salt bridge between the retinal Schiff base of Lys<sup>296</sup> and its counterion Glu<sup>113</sup> is broken, causing a shift in the absorption wavelength maximum of the visual pigment.<sup>51</sup> In analogy with bacteriorhodopsin, the photoreceptor can be viewed as a blocked proton pump.<sup>29</sup> Evidently any consideration of the energetics must include the contribution of the membrane bilayer.<sup>17</sup> As a result, flash photolysis has been used to address the role of the membrane lipids in generating fully functional rhodopsin as a paradigm for GPCRs in general.<sup>3,13,14,17,52,53</sup>

Much interest is currently focused on the biophysical properties of lipid membranes containing photoreceptors and other proteins that explain their natural selection and metabolic tight regulation with respect to key biological functions.<sup>54–56</sup> Lipid influences have been demonstrated for integral membrane proteins,<sup>57–60</sup> membrane-embedded peptides,<sup>61–63</sup> in eukaryotes,<sup>64</sup> and in microorganisms.<sup>1,65–68</sup> However, it is mainly for rhodopsin that lipid modulation of the conformational energetics of an integral membrane protein linked to function has been demonstrated in real time. To further test our proposal that material properties are involved in biomembrane functions,<sup>17</sup> rhodopsin was recombined with natural egg PC,<sup>22</sup> and flash photolysis studies were conducted under various experimental conditions, as a function of both pH and temperature. We wanted to prepare an artificial membrane recombinant using egg PC as a reference system because it contains only a neutral headgroup, together with a mixture of unsaturated acyl chains. Recombinants with a single phospholipid type are the basis of testing our hypothesized model that the electrostatic and other physical properties of the membrane lipids are involved in the functionality of rhodopsin. Comparison to the ROS membranes, with a mixture of phospholipid types, then allows one to probe the basis of the full activity in the native system.

- (41) Weitz, C. J.; Nathans, J. *Neuron* **1992**, *8*, 465–472.  
 (42) Gibson, S. K.; Parkes, J. H.; Liebman, P. A. *Biochemistry* **1998**, *37*, 11393–11398.  
 (43) Nathans, J. *Biochemistry* **1990**, *29*, 937–942.  
 (44) Khorana, H. G. *J. Biol. Chem.* **1992**, *267*, 1–4.  
 (45) Hubbell, W. L.; Cafiso, D. S.; Altenbach, C. *Nat. Struct. Biol.* **2000**, *7*, 735–739.  
 (46) Baldwin, J. *EMBO J.* **1993**, *12*, 1693–1703.  
 (47) Lomize, A. L.; Pogozheva, I. D.; Mosberg, H. I. *J. Comput.-Aided Mol. Des.* **1999**, *13*, 325–353.

- (48) Birge, R. R. *Annu. Rev. Phys. Chem.* **1990**, *41*, 683–733.  
 (49) Kochendoerfer, G. G.; Mathies, R. A. *J. Phys. Chem.* **1996**, *100*, 14526–14532.  
 (50) Cooper, A. *Curr. Opin. Chem. Biol.* **1999**, *3*, 557–563.  
 (51) Cohen, G. B.; Oprian, D. D.; Robinson, P. R. *Biochemistry* **1992**, *31*, 12592–12601.  
 (52) Mitchell, D. C.; Niu, S. L.; Litman, B. J. *J. Biol. Chem.* **2001**, *276*, 42801–42806.  
 (53) Niu, S. L.; Mitchell, D. C.; Litman, B. J. *J. Biol. Chem.* **2001**, *276*, 42807–42811.  
 (54) Brown, M. F.; Gibson, N. J. In *Essential Fatty Acids and Eicosanoids*, Sinclair, A., Gibson, R., Eds.; American Oil Chemists' Society Press: Champaign, 1992; pp 134–138.  
 (55) Litman, B. J.; Mitchell, D. C. *Lipids* **1996**, *31*, S193–S197.  
 (56) Moriguchi, T.; Greiner, R. S.; Salem, N. *J. Neurochem.* **2000**, *75*, 2563–2573.  
 (57) Navarro, J.; Toivio-Kinnucan, M.; Racker, E. *Biochemistry* **1984**, *23*, 130–135.  
 (58) Jensen, J. W.; Schutzbach, J. S. *Biochemistry* **1988**, *27*, 6315–6320.  
 (59) Lee, A. G. *Prog. Lipid Res.* **1991**, *30*, 323–348.  
 (60) Lee, A. G. *Curr. Biol.* **2000**, *10*, R377–R380.  
 (61) Keller, S. L.; Bezrukov, S. M.; Gruner, S. M.; Tate, M. W.; Vodyanoy, I.; Parsegian, V. A. *Biophys. J.* **1993**, *65*, 23–27.  
 (62) Epand, R. M. *Biochim. Biophys. Acta* **1998**, *1376*, 353–368.  
 (63) Lundbaek, J. A.; Andersen, O. S. *Biophys. J.* **1999**, *76*, 889–895.  
 (64) Kinnunen, P. *Chem. Phys. Lipids* **1996**, *81*, 151–166.  
 (65) Rietveld, A. G.; Chupin, V. V.; Koorengevel, M. C.; Wienk, H. L. J.; Dowhan, W.; de Kruijff, B. *J. Biol. Chem.* **1994**, *269*, 28670–28675.  
 (66) Morein, S.; Andersson, A. S.; Rilfors, L.; Lindblom, G. *J. Biol. Chem.* **1996**, *271*, 6801–6809.  
 (67) Karlsson, O. P.; Rytomaa, M.; Dahlqvist, A.; Kinnunen, P. K. J.; Wieslander, A. *Biochemistry* **1996**, *35*, 10094–10102.  
 (68) Andersson, A.-S.; Rilfors, L.; Orädd, G.; Lindblom, G. *Biophys. J.* **1998**, *75*, 2877–2887.

Previous work has investigated the contributions of the various headgroups present in the ROS disk membranes, including PE and PS, to the photochemistry of rhodopsin.<sup>14</sup> Related studies of light-induced reorganization of phospholipids in native rod disk membranes have been reported by Hofmann and co-workers.<sup>69</sup> The combined influences of the lipid polar headgroups and acyl chains point to a role of material properties of the membrane bilayer.<sup>17</sup> Within this framework, earlier results for negatively charged lipids such as PS suggest that although the  $\text{H}_3\text{O}^+$  ions in the electrical double layer are important, they are not the only factor that governs formation of metarhodopsin II,<sup>18</sup> as neutral PE headgroups and polyunsaturated DHA chains also promote meta II formation.<sup>10</sup> Here we have monitored titration curves for the meta I–meta II equilibrium at the same bulk and local pH values, obtained by applying the Gouy–Chapman model.<sup>30,31,70</sup> Analysis of the data for both the egg PC and the ROS membrane systems allows separation of the charge effects due to the concentration of hydronium ions,  $\text{H}_3\text{O}^+$ , in the electrical double layer<sup>14</sup> from the intrinsic charge effects on the bilayer properties. The results for the egg PC recombinants as compared to the native ROS membranes imply a significant functional role for properties associated with both the negatively charged PS headgroups, as well as the neutral lipid headgroups, plus the polyunsaturated DHA chains.

**Biophysical Properties of Membrane Lipids in Relation to Rhodopsin Function.** The experiments discussed here indicate that variation in the membrane composition<sup>14,71</sup> can govern the conformational transitions of rhodopsin important for the molecular mechanism of visual excitation.<sup>9,29</sup> Our analysis of the data for the ROS membranes in this work has considered both an asymmetric charge distribution, as well as a scrambled (symmetric) model, where the asymmetry of the protein and lipid components is lost. Similar conclusions are reached in each case, and in this regard the findings are independent of the detailed electrostatic model employed. An important feature is that the lipid influences are due to alteration of a thermodynamically reversible equilibrium between meta I and meta II, rather than any irreversible change in the activity of the protein. The flash photolysis titration curves demonstrate that the meta I–meta II transition of rhodopsin in both the egg PC recombinant as well as the native ROS membranes can be shifted by changes in both pH and temperature, consistent with an acid–base equilibrium. For instance, in the egg PC recombinant, the effect of the lipid composition is quite significant near room temperature and neutral pH, but not in the case of high or low pH. Moreover, by increasing the temperature of the egg PC recombinant membranes, one can similarly compensate for the influences of the bilayer lipid composition on the meta I–meta II equilibrium. The alterations in the photochemical behavior reveal there is an intrinsic difference in the thermodynamic state variables for the meta I–meta II transition in the two membrane systems.<sup>14</sup> On the basis of the comparison to the thermodynamic parameters for denaturation of compact globular proteins,<sup>72</sup> the results imply a partial unfolding of the rhodopsin molecule at the meta II stage of photolysis. Evidently properties of the lipid bilayer are of sufficient magnitude to

account for the free energy shifts of the meta I–meta II equilibrium.<sup>14</sup>

**Contribution of Membrane Electrostatics to the Meta I–Meta II Transition.** In this work, we have further investigated how electrostatic properties due to the membrane lipid–water interface modulate the formation of meta II. The principal charged phospholipid in the retinal rod membranes is PS, which can lead to alteration of the local pH at the membrane surface.<sup>18,73</sup> How can we explain the influences of PS in the native ROS membranes, which also contain PC and PE headgroups as well as polyunsaturated DHA chains? Clearly, the presence of the acidic phosphoserine headgroups may affect the meta I–meta II transition<sup>20</sup> due to titration of the amphoteric membrane surface. The influences of PS headgroups indicate that the membrane surface potential contributes to formation of meta II by increasing the local concentration of hydronium ions ( $\text{H}_3\text{O}^+$ ), driving the process toward completion (as a consequence of Le Châtelier's principle).<sup>73</sup> A negative membrane surface potential will cause an accumulation of protons and other cations within the diffuse electrical double layer. Hence, the value of the *apparent*  $\text{pK}_a$  measured for the flash photolysis data differs from the value of the *intrinsic*  $\text{pK}_a$ , due to the greater hydronium ion concentration at the membrane surface caused by the negatively charged headgroups of PS. Similar considerations apply to the pH dependence of the reaction kinetics. The importance of maintaining an optimal membrane surface potential ( $\psi_0$ ) is reflected in the fact that the native ROS membranes and recombinants containing PS display a significant increase in meta II production relative to the egg PC recombinants. As a result, the acid–base equilibrium can be driven to the meta II state by maintaining the concentration of hydronium ions relatively high at the surface of the membrane.

An interesting result of this work is that the  $\text{H}_3\text{O}^+$  ions in the electrical double layer, due to the membrane surface potential of PS, can largely explain the difference in the apparent  $\text{pK}_a$  for the meta I–meta II transition of rhodopsin in the ROS membranes versus the rhodopsin/egg PC recombinant membranes. In terms of the local pH, assuming a two-state transition, an intrinsic  $\text{pK}_a$  value of about 6.6 is obtained for both systems, consistent with protonation either of a histidine residue<sup>41</sup> or possibly Glu<sup>134</sup> of rhodopsin.<sup>74,75</sup> Previous lipid substitution experiments<sup>10,17</sup> have shown that PE headgroups and/or neutral DHA chains are also capable of promoting formation of the activated meta II state; that is, they both lead to an increase in the apparent  $\text{pK}_a$ . One would expect the influences of the PE plus DHA to also be expressed when the ROS membranes are compared to the rhodopsin/egg PC recombinants at the same *local* pH values. Yet this is contrary to experimental observation, where similar *intrinsic*  $\text{pK}_a$  values are observed in both cases. It follows that the meta II-promoting effects of the PE headgroups and DHA chains are counteracted by the intrinsic bilayer influences of PS in the ROS membranes, which are independent of the  $\text{H}_3\text{O}^+$  activity. This proposal explains the lack of increased meta II formation in the ROS membranes versus the reference egg PC recombinant at the same surface

(69) Hessel, E.; Müller, P.; Herrmann, A.; Hofmann, K. P. *J. Biol. Chem.* **2001**, *276*, 2538–2543.

(70) McLaughlin, S. *Annu. Rev. Biophys. Biophys. Chem.* **1989**, *18*, 113–136.

(71) Botelho, A. V.; Gibson, N. J.; Wang, Y.; Thurmond, R. L.; Brown, M. F. *Biophys. J.* **2001**, *80*, 547a.

(72) Privalov, P. L.; Gill, S. J. *Adv. Protein Chem.* **1988**, *39*, 191–234.

(73) Gibson, N. J.; Brown, M. F. *Photochem. Photobiol.* **1991**, *54*, 985–992.

(74) Arnis, S.; Fahmy, K.; Hofmann, K. P.; Sakmar, T. P. *J. Biol. Chem.* **1994**, *269*, 23879–23881.

(75) Cohen, G. B.; Yang, T.; Robinson, P. R.; Oprean, D. D. *Biochemistry* **1993**, *32*, 6111–6115.

pH. Apparently nature has selected PS as a means of generating a high  $[H_3O^+]$  in the electrical double layer adjacent to the membrane surface, corresponding to a local pH less than that of the cytosol, thus governing the amount of meta II. Paradoxically, the influences of PS on the *intrinsic* bilayer properties (see below) oppose meta II formation and must be overcome by the additional presence of PE headgroups and DHA chains. Thus, *both* PS together with PE and DHA chains are needed for full meta II production. If correct, this proposal would explain the role of lipid diversity in the ROS membrane system containing rhodopsin.

**Role of Bilayer Material Properties.** What are the bilayer properties that influence the conformational energetics of integral membrane proteins such as rhodopsin? As a rule, they can include the solvation energy of the lipid/protein interface,<sup>12,14</sup> the elastic curvature and/or area stress/strain of the bilayer lipids,<sup>10,14</sup> and the electrostatic potential of the membrane.<sup>14,20,76</sup> The interaction between rhodopsin and the lipids within the hydrocarbon region of the bilayer can be represented by a lipid–protein interfacial tension. The interfacial tension ( $\gamma_{LP}$ ) is a measure of the energy of solvating the protein intramembraneous surface by the hydrocarbon region of the bilayer.<sup>12,14,17</sup> This results in a pressure differential which exists across a curved interface, the so-called *Laplace pressure*. The variation of the pressure treated by the Laplace equation is related to the two principal radii of curvature. In the case of a cylindrical intramembraneous shape, one of the curvature radii becomes infinite, and the Laplace pressure is inversely proportional to the protein radius ( $r$ ), as given by  $\Delta P = \gamma_{LP}/r$ . Hence changes in the protein structure may correspond to surface work, involving an alteration of the lipid–protein interface.<sup>17</sup> As rhodopsin is embedded in the bilayer by the protein/lipid interfacial tension and is stabilized in the dark, any structural variation, either from the protein or from the lipid, can affect the force balance. Generally, the free energy due to the lipid–protein interface is balanced by other contributions, that is, due to the elastic area stress involving the lipid–water interface, or the curvature stress of the individual opposed monolayers of the membrane.<sup>14</sup> The lateral stress of the membrane lipids may have similar values for the whole bilayer (as in the case of egg PC which forms the planar  $L_\alpha$  phase), or there may be different values at various depths within the bilayer.<sup>77</sup> Equivalently, the thermodynamic properties of the membrane can include a contribution from the spontaneous curvature associated with the lipid/water interface, a key structural property of the bilayer.<sup>17</sup>

In previous work,<sup>3,17</sup> we have emphasized the importance of the combined influences of the membrane lipid headgroups and acyl chains<sup>10</sup> in terms of a *flexible surface model*, involving curvature elastic deformation<sup>78,79</sup> of the membrane. We have proposed that the meta I–meta II transition is coupled to a change in the membrane curvature elastic stress, as given by the Helfrich<sup>78</sup> bending energy

$$g_c = \kappa(H - H_0)^2 + \bar{\kappa}K \quad (24)$$

In the above formula,  $\kappa$  is the force constant (bending rigidity),  $H$  is the actual monolayer curvature of the membrane,  $H_0$  is

the natural or spontaneous curvature,  $\bar{\kappa}$  is the modulus of Gaussian curvature, and  $K$  is the product of the two principal curvatures. According to this new paradigm, the meta I state is favored by lipids tending to form the *lamellar* phase ( $L_\alpha$ ), having a planar/water interface as in the case of egg PC. Thus, lipids with zero spontaneous curvature favor the meta I state. By contrast, the meta II state is favored by lipids with a propensity to form *nonlamellar* phases in the absence of protein,<sup>71</sup> for example, reverse hexagonal ( $H_{II}$ ) nanostructures,<sup>79</sup> in which the membrane aqueous interface curls toward water. Lipids with a negative spontaneous curvature stabilize the meta II state, that is, by having small headgroups in combination with bulky acyl chains, which lead to a wedge-like “average shape”.<sup>80</sup> Because PE headgroups and/or polyunsaturated DHA chains promote meta II formation,<sup>10,14</sup> it follows that the elastic stress/strain due to membrane deformation can contribute to the energetics of the meta I–meta II transition, involving curvature frustration of the bilayer.<sup>10,14</sup> Thermodynamic analysis indicates that the material properties associated with the bending energy of the flexible membrane surface are of sufficient magnitude to govern the meta I–meta II transition, thus providing a novel means of free energy coupling of the bilayer lipids to the protein.<sup>14</sup>

As discussed above, for membranes containing PS or other charged lipid constituents, one needs to separate the intrinsic influences on the bilayer free energy from the electrostatic influences due to the electrical double layer. On account of the negative surface charge density of PS, there are two possible contributions that can oppose or reinforce each other: (i) As already noted, the surface charge can alter the concentration of hydronium ions,  $H_3O^+$ , in the electrical double layer, thereby affecting the meta I–meta II equilibrium due to the proton uptake and favoring *meta II*. In this case, the effects of the positive and negative surface charge density on meta II formation are expected to be essentially opposite. (ii) In addition, the surface charge due to PS (independent of charge sign, viz.,  $\pm$ ) is expected to lead to a *decrease* in the spontaneous curvature  $H_0$ , favoring the planar bilayer ( $L_\alpha$ ) state ( $H_0 = 0$ ), that is, favoring the *meta I* state irrespective of the sign of the surface charge. It is known that PS tends to form the lamellar ( $L_\alpha$ ) phase, having a planar lipid/water interface, in contrast to the influences of PE plus DHA chains. Given a flexible surface model, the effect of the surface charge on the spontaneous curvature  $H_0$  opposes the influence of  $H_3O^+$  ions in the electrical double layer, so that the meta II/meta I ratio is a balance of two opposing tendencies. Thus, the charge influences of PS can involve an interplay between the local pH and its effects on the free energy of curvature deformation of the ROS membranes. We note that the effects of screening the surface charge by addition of salt can alter both of the above contributions. The ionic strength will affect the hydronium ion concentration in the electrical double layer, shifting the equilibrium toward the left, in the direction of meta I. Yet screening the surface charge density can also lead to a more negative spontaneous curvature  $H_0$ , inasmuch as less energy is needed to deform a given monolayer film of the bilayer. The influence of the surface charge on the spontaneous curvature  $H_0$  is *opposite* to the effect on the  $H_3O^+$  concentration. Thus, for both negative and positive surface charge density, this effect of ionic strength will favor meta II.

(76) Cafiso, D. S.; Hubbell, W. L. *Photochem. Photobiol.* **1980**, *32*, 461–468.

(77) Cantor, R. S. *J. Phys. Chem. B* **1997**, *101*, 1723–1725.

(78) Helfrich, W. *Z. Naturforsch.* **1973**, *28c*, 693–703.

(79) Gruner, S. M. *J. Phys. Chem.* **1989**, *93*, 7562–7570.

(80) Israelachvili, J. N. *Intermolecular and Surface Forces*, 2nd ed.; Academic Press: San Diego, 1992.

These opposite influences of ionic strength may help explain previous studies of salt effects on the meta I–meta II transition of the PS-containing native ROS membranes.<sup>18</sup>

Thus, a new feature of the present work is that PS headgroups can essentially antagonize the meta II-promoting effect of the PE headgroups plus DHA chains.<sup>10,14</sup> We propose that *both* PS headgroups and the combination of PE plus DHA chains are needed, that is, sufficient, for full meta II formation in the ROS membranes. By contrast, neither class of lipids alone is sufficient.<sup>10,14</sup> If the membrane contained only PC plus PS, then the  $\text{H}_3\text{O}^+$  ions in the electrical double layer would favor meta II, but this would be counteracted by the deformation energy of the charged bilayer surface. Consequently, nature has selected lipids with a highly negative spontaneous curvature to overcome the  $\sim$  zero spontaneous curvature of PC and PS. The typical levels of PE in mammalian cells are insufficient to reverse the bilayer-stabilizing effect of PS. Highly polyunsaturated DHA chains<sup>81,82</sup> are also required to provide the additional curvature stress needed for full rhodopsin photochemical function. It follows that PS provides the  $\text{H}_3\text{O}^+$  ions in the electrical double layer, and the PE plus DHA chains give the requisite large negative spontaneous curvature. The  $\text{H}_3\text{O}^+$  ions, as well as phosphorylation of rhodopsin,<sup>19,42</sup> represent possible controlling elements of the visual process at the initial amplification stage, leading to a variable gain. We also propose that the interplay of the electrostatic influences on the ionic composition of the electrical double layer with the deformation energy of the membrane accounts for the lipid diversity of the ROS membranes, and perhaps other receptor systems as well.

Finally, we emphasize that the conclusions implicated in this work come from flash photolysis data acquired for the protein and that we are not studying the bilayer directly, for example, using solid-state NMR spectroscopy.<sup>83</sup> The results cannot be fully interpreted as a generalization for the role of the bilayer

in the ROS membranes. Our conclusions remain open to further investigation, since new techniques and approaches may eventually allow the kinetics and the structures of each of the intermediates involved in the rhodopsin transients to be investigated, thereby contributing to a greater understanding of the role of the lipid bilayer. Formation of meta II with subsequent binding of the G protein, transducin, provides a specific paradigm for understanding how the GPCRs function, where any interactions with the membrane bilayer have specific mechanistic consequences. By comparing flash photolysis data for the egg PC recombinant and ROS membrane samples, this work has contributed to identification of the physical properties of lipids modulating the function of the protein, including a role for PS, PE, and DHA in formation of the activated meta II state. We anticipate that our findings will continue to stimulate new thinking in chemical biology and more experiments regarding the rhodopsin-lipid recombinants. In future studies, it will be interesting to determine the relative magnitudes of the headgroup and polyunsaturation contributions to the energetics of the bilayer deformation, the curvature stress in the membrane, as well as the role of electrostatic properties of the bilayer lipids. Rhodopsin has been shown to interact with the bilayer membrane through various physical interactions, but the functional significance has not yet been completely established, and future work remains to be done.

**Acknowledgment.** This research was supported by the U. S. National Institutes of Health. A.V.B. is the recipient of a scholarship from CAPES, Brasilia, D.F., Brazil, and G.V.M. is a Postdoctoral Fellow of the U.S. NIH. We are grateful to Nicholas Gibson for his assistance, and to Gordon Tollin and Thomas Huber for many valuable discussions during the course of this work.

JA0200488

(81) Huber, T.; Rajamoorthi, K.; Kurze, V. F.; Beyer, K.; Brown, M. F. *J. Am. Chem. Soc.* **2002**, *124*, 298–309.

(82) Petrache, H.; Salmon, A.; Brown, M. F. *J. Am. Chem. Soc.* **2001**, *123*, 12611–12622.

(83) Brown, M. F. In *Biological Membranes*; Merz, K. M., Jr., Roux, B., Eds.; Birkhäuser: Basel, 1996; pp 175–252.